# An Analysis of Photon Beam Characteristics of a LINAC in Water Phantom

[1]Chowdhury M. R. I. , [2]Rahman M. M. , [3]Rabby M. F.

**Abstract**

*The use of linear accelerators with megavoltage photon beams in radiation therapy provides more accurate dosage delivery. It is usually used to destroy cancer cells. It is important to analyze the every aspects of the delivered beam thoroughly, including the PDD, beam profile, output factor, etc before using linear accelerators for clinical purposes. The purpose of this work is to enhance the quality of radiation treatment planning by analyzing the photon beam PDD and profiles (penumbra width, symmetry, and beam flatness) for different beam energies. A Varian LINAC (SN: 5199) was used for these measurements at the TMSS Cancer Center in Bogura, Bangladesh, with photon energies of 6 MV, 10 MV, and 15 MV. The depth dose, penumbra, symmetry, and flatness of photon beams do not exhibit a linear relationship since beam quality mostly depends on how photons interact with matter. Due to scattering by matter, photon attenuation and penetration characteristics vary with dosimetric parameters such as field size, source to surface distance, etc. When a wide range of beam energies are available, a comprehensive analysis of photon properties assists in choosing the relevant beam for radiation treatment.*

**Keywords:** Build-up region, PDD, Penumbra, Symmetry, Flatness, LINAC, etc

## 1. Introduction

Megavoltage energy used in radiotherapy treatments, if not properly planned, this could result in treatment errors and put patients at risk.[1] Medical LINAC is the machine to deliver the megavoltage energy in form of photon and electron beams. In order to choose the best set of treatment planning parameters, it is necessary to determine the dosimetric characteristics of the radiation beams before using this megavoltage energy for clinical purposes.[2]

A dose computation method designed to forecast dose distribution in a real patient uses data on dose distribution that is nearly exclusively obtained from measurements in phantoms. These tissue equivalent phantoms are made using various materials and methods.[3, 4] Radiation physicists use measured dosimetry data to optimize treatment plans and calculate doses for specific plans. In reality, this data represents dosimetric quantities that depict various physical properties of the machine, beam, and its energies.

For photon beam energies of 6 MV, 10 MV, and 15 MV, this study evaluated the

[1] *Department of Computer Science & Engineering, Pundra University of Science & Technology.*

[2, 3] *Department of Radiation Oncology Physics, TMSS Cancer Center, Bogura, Bangladesh.*

*Corresponding Email: riadul.mric@gmail.com*

fundamental dosimetric parameters, including percentage depth dose (PDD) and beam profile characteristics such as symmetry, flatness, and penumbra, across different depths and field sizes. PDD is defined as the percentage of the absorbed dose at a given depth relative to the dose at a reference depth.[5] Beam symmetry refers to the variation in the distances, measured between the left and right sides, from the central axis point at the 50% dose level to the dose points on a beam profile. Flatness refers to the variation in dose intensity across the central 80% of the beam width of the beam profile, typically evaluated at 10 cm depth in a plane perpendicular to the central axis.[6] On the other hand, penumbra is defined as the lateral distance between the 80% and 20% dose points on a transverse beam profile measured in a water phantom.[10] All measurements were performed using a Varian linear accelerator (LINAC) equipped with a 3D computer-controlled water phantom at the TMSS Cancer Center in Bogura, Bangladesh.

## 2. Materials and Method

This study was conducted using a dual-energy linear accelerator (Varian VitalBeam, SN: 5199), capable of delivering photon energy beams of 6 MV, 10 MV, 15 MV, and 6 MV FFF, as well as electron energy beams of 4 MeV, 9 MeV, 12 MeV, 15 MeV, and 18 MeV. Dosimetric measurements for the 6 MV, 10 MV, and 15 MV photon energy beams were performed using a 3D computer-controlled water phantom equipped with a CC13 ionization chamber (SN: 18616) as the field chamber and a CC04 ionization chamber (SN: 18635) as the reference chamber. Data acquisition and analysis were carried out using the IBA myQA Accept software. The PDDs were obtained over a range of depths and field sizes (4 × 4, 6 × 6, 8 × 8, 10 × 10, 12 × 12, 15 × 15, 20 × 20, 30 × 30, and 40 × 40 $cm^2$) keeping SSD at 100 cm. Beam profile analysis included the assessment of symmetry, flatness, and penumbra width were obtained for various field sizes (4 × 4, 10 × 10, and 20 × 20 $cm^2$) and depths. Furthermore, utilizing the Eclipse, an external treatment planning system, the calculations of PDDs and beam profiles were carried out.

## 3. Results and Discussion

As radiation beam passes through a medium, attenuation takes place and the dose deposited (usually described as PDD) varies with respect to the depth, field size, energy and SSD.

### 3.1. Central Axis PDD

The central axis PDDs in water were computed for field sizes from 4 × 4 $cm^2$ to 40 × 40 $cm^2$ at 100 cm SSD. It is observed that the PDD builds up rapidly with depths for first few centimeters and progressively attains its peak value at a certain depth. As the secondary electrons must travel a distance before depositing dose, the maximum dose deposited at some depth from the surface. For 6 MV photon beam, the PDD increases from 50.7% to 90.1% in the first 6 mm and attains its peak value at 15 mm depth for 10 × 10 $cm^2$ field size. Similarly the peak values occur at 24 mm and 29 mm for 10 MV and 15 MV photon beams with 10 × 10 $cm^2$ field size respectively. Beyond the depth of maximum dose, PDD decreases with depth in a nonlinear fashion. This is because of the inverse square law and the modes of interaction of beams with matter vary significantly with the different beam parameters. It is also observed that the depth of peak dose decreases with increase of field sizes because larger field size increases backscattering of photon beam. The maximum dose were achieved for various field sizes at depth (14.5-16.0) mm, (18.0-25.0) mm and (19.5-29.50) mm with 6 MV, 10 MV and 15 MV photon beams respectively. Again PDD increases with field sizes because of backscattering of photon beam.[11] The PDDs for various depths and field sizes are presented in Table-1 to Table-3 and the corresponding PPD build-up curves are shown in Figure-1 to Figure-4, for 6 MV, 10 MV and 15 MV photon energy levels respectively.

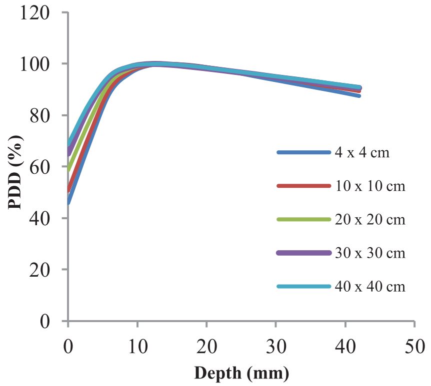


**Figure 1:** PDD build-up curves with 6 MV photon beam with various field sizes.

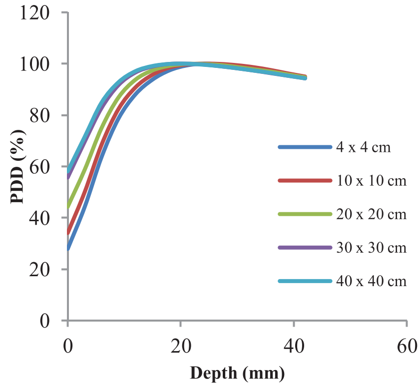


**Figure 2:** PDD build-up curves with 10 MV photon beam with various field sizes.

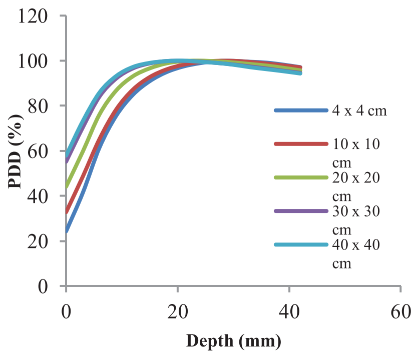


**Figure 3:** PDD build-up curves with 15 MV photon beam with various field sizes.

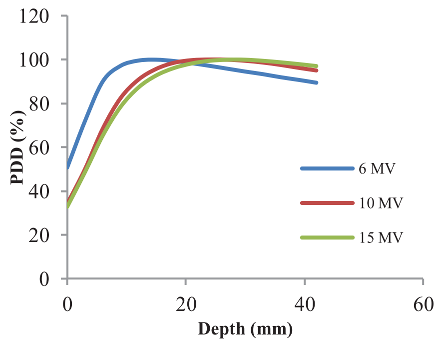


**Figure 4:** PDD build-up curves with 10 × 10 $cm^2$ field size for different photon beams.

For 10 × 10 field size we found that an average rise of doses per cm are 31.7%, 27.5% and 23.5% until the $d_{max}$ are reached and beyond the $d_{max}$ the average decline of doses per cm are 2.69%, 2.53% and 2.46% with 6 MV, 10 MV and 15 MV photon energies respectively. Again with field size of 10×10 $cm^2$, the average dose drops between the depths of the peak dose and depths of the 50% dose per centimeter were determined 3.67%, 3.11%, and 2.91% for 6 MV, 10 MV and 15 MV photon beam respectively. Thus, as the beam energy increases, the dosage drop per centimeter between these two depths ($d_{max}$ to $d_{50}$) decreases. Figure-6 shows the comparative variation between $d_{max}$ and $d_{50}$ for photon beams which indicates how the disparity between these depths grows with increasing beam energy. Thus it is evident that from surface to $d_{max}$ and beyond the $d_{max}$ the amount of deposited dose per cm decreases with increasing beam energy though beyond $d_{max}$ the amount of deposited dose increase with increasing energy. Higher energy beams provide a greater dose at depth because they have more penetrating power. Figure-8 shows that the surface dose will decrease while $d_{max}$ increases with increase of energy. The relationship among these is obvious but do not have linear relationship because the mode of interaction with matter differs quite significantly with respect to beam energy.[7, 8, 9]

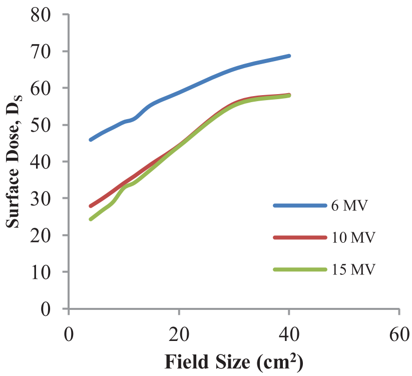


**Figure 5:** The fluctuation of surface dose for different field sizes.

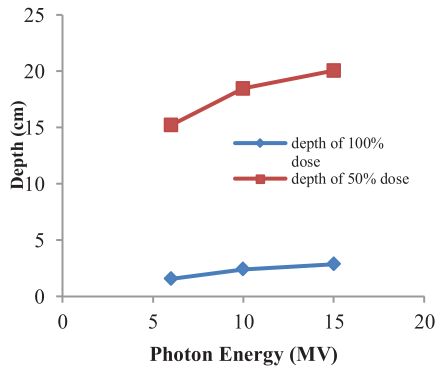


**Figure 6:** The fluctuation of depth of maximum dose and 50% dose with photon energy.

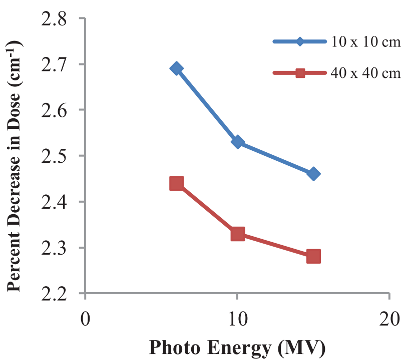


**Figure 7:** Average decrease in dose beyond $d_{max}$ for different photon beams.

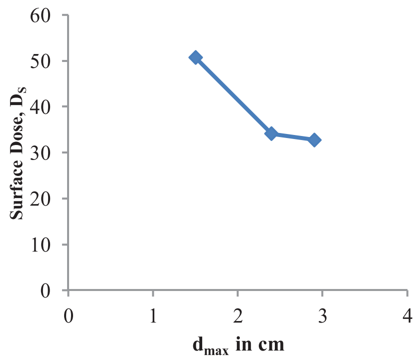


**Figure 8:** The variation of surface dose with $d_{max}$.

**TABLE 1: Measured PDDs for 6 MV photon energy with various field sizes in water phantom.**

| Depth (cm) | Field Size ($cm^2$) | | | | | | | | |
|---|---|---|---|---|---|---|---|---|---|
| | (4 × 4) | (6 × 6) | (8 × 8) | (10 × 10) | (12 × 12) | (15 × 15) | (20 × 20) | (30 × 30) | (40 × 40) |
| 0.0 | 45.9 | 47.7 | 49.2 | 50.7 | 51.7 | 55.4 | 58.7 | 65.1 | 68.7 |
| 0.6 | 88.5 | 88.9 | 89.3 | 90.1 | 89.7 | 92.2 | 92.5 | 94.9 | 95.3 |
| 1.2 | 99.5 | 99.4 | 99.5 | 99.5 | 99.5 | 99.8 | 99.7 | 99.9 | 99.9 |
| 1.5 | 99.9 | 99.9 | 100 | 99.9 | 99.9 | 99.9 | 99.8 | 99.6 | 99.8 |
| 2.1 | 98.2 | 98.3 | 98.2 | 98.3 | 98.3 | 98.2 | 97.9 | 97.9 | 98.1 |
| 3.0 | 93.6 | 94.1 | 94.4 | 94.5 | 94.7 | 94.7 | 94.7 | 94.8 | 95.1 |
| 4.5 | 86.1 | 87.1 | 87.7 | 88.2 | 88.6 | 88.7 | 89.1 | 89.5 | 90.1 |
| 7.5 | 71.8 | 73.6 | 74.9 | 75.8 | 76.6 | 77.3 | 78.1 | 79.2 | 79.9 |
| 9.0 | 65.5 | 67.5 | 68.9 | 70.1 | 71.1 | 71.9 | 72.9 | 74.2 | 75.1 |
| 15.0 | 45.3 | 47.3 | 49.2 | 50.4 | 51.7 | 52.9 | 54.6 | 56.6 | 57.7 |
| 18.0 | 37.7 | 39.6 | 41.2 | 42.7 | 43.9 | 45.2 | 47.1 | 49.2 | 50.4 |
| 24.0 | 26.4 | 27.9 | 29.3 | 30.6 | 31.7 | 33.2 | 34.7 | 36.9 | 38.1 |
| 27.0 | 22.2 | 23.5 | 24.7 | 25.9 | 26.9 | 28.2 | 29.8 | 31.9 | 33.1 |
| 30.0 | 18.7 | 19.8 | 21.2 | 22.2 | 22.9 | 24.1 | 25.6 | 27.6 | 28.8 |

**TABLE 2: Measured PDDs for 10 MV photon beam with various field sizes in water phantom.**

| Depth (cm) | Field Size ($cm^2$) | | | | | | | | |
|---|---|---|---|---|---|---|---|---|---|
| | (4 × 4) | (6 × 6) | (8 × 8) | (10 × 10) | (12 × 12) | (15 × 15) | (20 × 20) | (30 × 30) | (40 × 40) |
| 0.0 | 27.9 | 29.8 | 31.9 | 34.1 | 36.1 | 39.3 | 44.3 | 55.7 | 58.1 |
| 0.6 | 63.7 | 65.2 | 66.6 | 68.5 | 69.7 | 72.1 | 75.1 | 82.8 | 84.9 |
| 1.2 | 88.1 | 89.2 | 89.8 | 90.8 | 91.4 | 92.5 | 93.8 | 96.6 | 97.1 |
| 2.4 | 100 | 100 | 100 | 100 | 100 | 100 | 99.9 | 99.7 | 99.6 |
| 3.0 | 98.9 | 99.3 | 99.2 | 99.4 | 99.6 | 98.9 | 98.7 | 98.2 | 98.2 |
| 4.5 | 93.1 | 93.8 | 93.8 | 93.9 | 93.8 | 93.8 | 93.5 | 93.3 | 93.3 |
| 6.0 | 86.6 | 87.5 | 88.1 | 88.2 | 88.1 | 88.3 | 88.2 | 88.4 | 88.4 |
| 9.0 | 74.7 | 76.1 | 76.8 | 77.2 | 77.6 | 78.2 | 78.5 | 78.7 | 79.1 |
| 12.0 | 64.2 | 65.8 | 66.8 | 67.6 | 67.9 | 68.7 | 69.6 | 70.1 | 70.5 |
| 15.0 | 55.1 | 56.9 | 58.1 | 58.8 | 59.4 | 60.4 | 61.5 | 62.1 | 62.5 |
| 18.0 | 47.3 | 49.1 | 50.3 | 51.2 | 51.9 | 52.8 | 54.1 | 54.9 | 55.4 |
| 24.0 | 35.3 | 36.9 | 38.1 | 38.8 | 39.5 | 40.7 | 41.9 | 42.9 | 43.5 |
| 27.0 | 30.4 | 32.2 | 33.1 | 33.8 | 34.5 | 35.8 | 36.8 | 37.8 | 38.4 |
| 30.0 | 26.2 | 27.7 | 28.7 | 29.2 | 29.8 | 31.3 | 32.1 | 33.3 | 34.7 |

**TABLE 3: Measured PDDs for 15 MV photon energy with various field sizes in water phantom.**

| Depth (cm) | Field Size ($cm^2$) | | | | | | | | |
|---|---|---|---|---|---|---|---|---|---|
| | (4 × 4) | (6 × 6) | (8 × 8) | (10 × 10) | (12 × 12) | (15 × 15) | (20 × 20) | (30 × 30) | (40 × 40) |
| 0.0 | 24.3 | 26.6 | 28.9 | 32.8 | 34.3 | 37.9 | 44.1 | 55.2 | 57.9 |
| 0.6 | 61.5 | 62.9 | 65.0 | 65.3 | 69.2 | 71.5 | 76.2 | 84.1 | 85.9 |
| 1.2 | 84.9 | 85.6 | 86.9 | 87.2 | 89.1 | 90.9 | 93.1 | 96.6 | 97.2 |
| 2.4 | 98.9 | 99.3 | 99.2 | 99.4 | 99.8 | 100 | 100 | 99.6 | 99.5 |
| 3.0 | 99.9 | 100 | 99.9 | 99.9 | 99.8 | 99.6 | 99.2 | 98.3 | 98.2 |
| 4.5 | 96.4 | 96.3 | 96.1 | 96.1 | 95.8 | 95.5 | 94.6 | 93.6 | 93.3 |
| 6.0 | 90.0 | 90.7 | 90.4 | 90.8 | 90.5 | 90.0 | 89.6 | 88.7 | 88.5 |
| 9.0 | 78.7 | 79.2 | 80.0 | 80.3 | 80.2 | 80.0 | 80.0 | 79.5 | 79.4 |
| 12.0 | 68.4 | 69.4 | 70.4 | 70.4 | 70.9 | 71.1 | 71.2 | 71.0 | 71.3 |
| 15.0 | 59.2 | 60.4 | 61.2 | 61.9 | 62.2 | 62.9 | 63.2 | 63.4 | 63.4 |
| 18.0 | 51.2 | 52.7 | 53.6 | 54.3 | 54.8 | 55.5 | 56.1 | 56.4 | 56.6 |
| 24.0 | 38.9 | 40.1 | 41.2 | 41.9 | 42.4 | 43.2 | 44.0 | 44.7 | 45.0 |
| 27.0 | 33.7 | 35.1 | 35.9 | 36.7 | 37.3 | 38.0 | 39.0 | 39.5 | 40.1 |
| 30.0 | 29.5 | 30.5 | 31.5 | 32.2 | 32.6 | 33.5 | 34.3 | 35.0 | 35.5 |

For photon energy 6 MV, 10 MV and 15 MV, the beam profile data and corresponding profile curves with various depth and field sizes are presented in Table-4, Table-5 and displayed in Figure-11 to Figure-11 respectively.

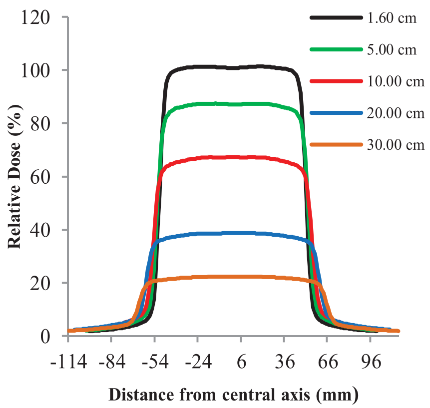


**Figure 9:** Profile doses curve for 6 MV photon beam at field size 10 x 10 $cm^2$ with various depth

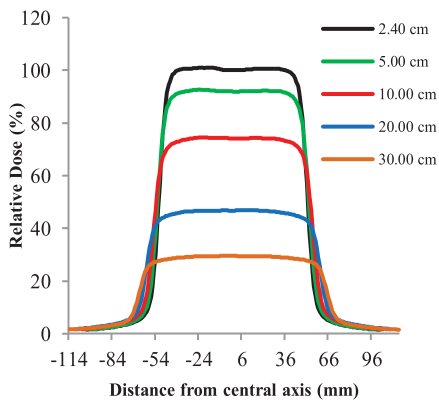


**Figure 10:** Profile doses curve for 10 MV photon beam at field size 10 x 10 $cm^2$ with various depth

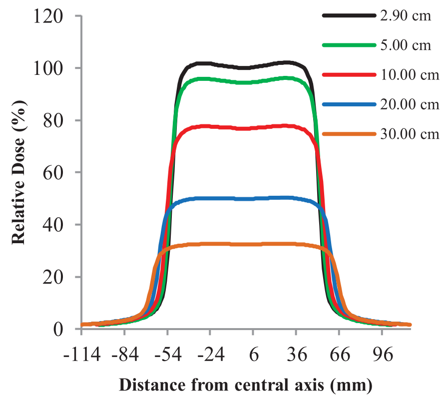


**Figure 11:** Profile doses curve for 15 MV photon beam at field size 10 x 10 cm$^2$ with various depth

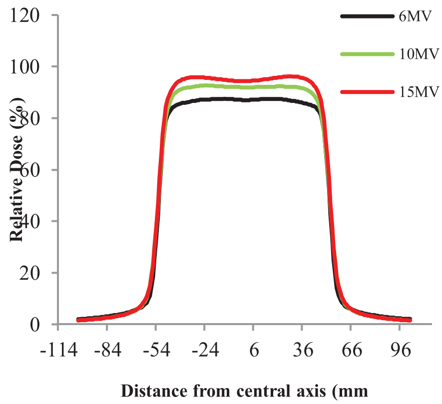


**Figure 12:** Profile doses curve for various photon beams at field size 10 x 10 cm$^2$ with 10 cm depth.

Our research founds that, beam profiles vary with energy due to changes in photon scattering. Higher energies tend to have narrower forward peaks, while lower energies are broader. The existence of photons with varying energies within the same energy beam causes the beam flatness to increase with depth as the photon beam's penetrating power decreases with depth. As the dispersion of photon beam increases with field size and the same beam is made up of photons with varying energy levels, beam flatness increases with field size. Because the energy difference among the photons in the same beam increases, flatness increases with beam energy. For photon energies of 6 MV, 10 MV, and 15 MV, the estimated beam flatness at 10 cm depth with field size 10 × 10 cm2 and SSD 100 cm are 2.51%, 2.62%, and 2.90% respectively.

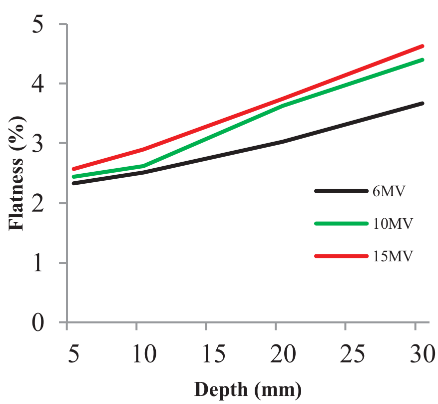


**Figure 13:** Variation of flatness with depth for different photon beams at field size 10x10 cm$^2$

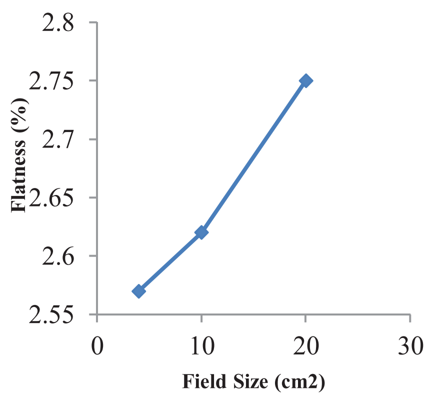


**Figure 14:** Variation of flatness with field sizes.

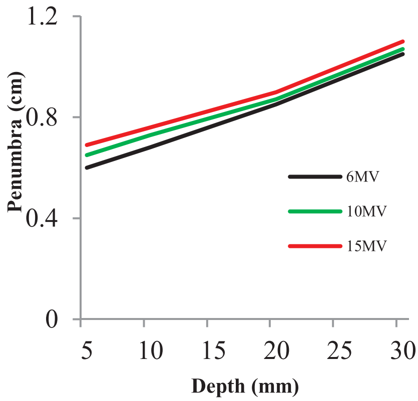


**Figure 15:** Variation of penumbra with depth for different photon beams with field size 10x10 cm$^2$

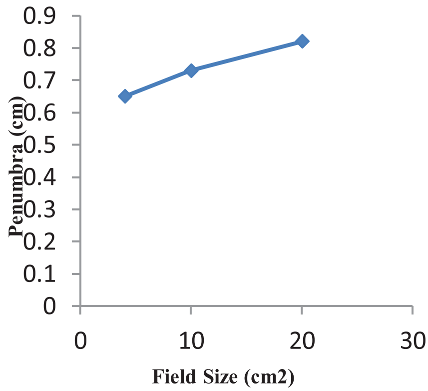


**Figure 16:** Variation of penumbra with field sizes.

As the field size and photon beam energy increase, the obliquity of the photon beam at the edges of the collimator opening also increases, resulting in a wider penumbra. The penumbra further increases with depth because the photon beam undergoes greater lateral dispersion with increasing depth. Since photon interactions with matter depend on multiple factors, the relationship between beam flatness and penumbra is complex and nonlinear. Therefore, the rates at which beam flatness and penumbra change do not increase linearly with increases in field size, depth, or beam energy.

**TABLE 4: Profile analysis of photon beams at field size 10 x 10 cm$^2$ with various depths.**

| Depth (cm) | Symmetry (%) | | | Flatness (%) | | | Penumbra (cm) | | |
|---|---|---|---|---|---|---|---|---|---|
| | 6 MV | 10 MV | 15 MV | 6 MV | 10 MV | 15 MV | 6 MV | 10 MV | 15 MV |
| 1.6 | 0.19 | - | - | 1.86 | - | - | 0.55 | - | - |
| 2.4 | - | 0.02 | - | - | 2.23 | - | - | 0.62 | - |
| 2.9 | - | - | 0.05 | - | - | 2.17 | - | - | 0.66 |
| 5.0 | 0.24 | 0.02 | 0.02 | 2.33 | 2.44 | 2.57 | 0.60 | 0.65 | 0.70 |
| 10.0 | 0.19 | 0.05 | 0.03 | 2.51 | 2.62 | 2.90 | 0.68 | 0.73 | 0.76 |
| 20.0 | 0.24 | 0.01 | 0.05 | 3.03 | 3.63 | 3.75 | 0.85 | 0.87 | 0.90 |
| 30.0 | 0.12 | 0.05 | 0.11 | 3.67 | 4.40 | 4.63 | 1.05 | 1.07 | 1.11 |

**TABLE 5: Profile analysis of photon beams at 10 cm depth with various field sizes.**

| Fields Size (cm2) | Symmetry (%) | | | Flatness (%) | | | Penumbra (cm) | | |
|---|---|---|---|---|---|---|---|---|---|
| | 6 MV | 10 MV | 15 MV | 6 MV | 10 MV | 15 MV | 6 MV | 10 MV | 15 MV |
| 4 × 4 | 0.23 | 0.25 | 0.01 | 1.66 | 2.57 | 2.81 | 0.59 | 0.65 | 0.69 |
| 10 × 10 | 0.19 | 0.05 | 0.03 | 2.51 | 2.62 | 2.90 | 0.69 | 0.73 | 0.76 |
| 20 × 20 | 0.04 | 0.10 | 0.03 | 2.65 | 2.75 | 2.97 | 0.81 | 0.82 | 0.84 |

On the other hand photon beam symmetry which measures the left-right profile uniformity is generally independent of field size and depth for standard, well-calibrated linear accelerators. It can actually change slightly with field size and depth due to the increasing predominance of scattered radiation compared to the primary beam, particularly in higher energy beams.

## 4. Conclusion

In order to enhance the accuracy, photon beam PDD and profile features analysis are important in radiotherapy treatment planning. Since every target volume and the tissues around it require a certain dose, radiotherapy should always provide the necessary dose distribution. Detailed analysis of properties of the absorbed dose in water relative to depths, field sizes and energy depicts the way in which dose decreases or increases at specific point. Our present study contains the knowledge of energy and the geometrical influence of different dosimetric parameters for absorbed dose calculation which will be helpful in choosing the appropriate planning for cancer treatment.

**Acknowledgments**

The authors express their humble gratitude to all the officers and employees at TMSS Cancer Center, Bogura, Bangladesh, for their cooperation in the research work.

**Conflicts of interest**

All the authors declare that they have no conflicts of interest.

## References

[1] IAEA 2008 Commissioning of Radiotherapy Treatment Planning Systems : Testing for Typical External Beam Treatment Techniques TECDOC 1583 IAEA TECDOC

[2] Mittal V K, Verma R C, Gupta S C, Introduction to nuclear and particle physics. 2nd ed. 2011;247.

[3] White D R, Martin R J, Darlison R. Epoxy resin based tissue substitutes. Br J Radiol 1977;50:814–21.

[4] International Commission on Radiation Units and Measurements. Tissue substitutes in radiation dosimetry and measurements, Report No. 44. Bethesda, MD: International Commission on Radiation Units and Measurements 1989.

[5] Podgorsak E B. Radiation oncology physics: a handbook for teachers and students. IAEA. 2005;103:370.

[6] Khan F M, Gibbons J P, The physics of radiation therapy. 5th ed.

[7] Rahman M, Shamsuzzaman M, Sarker M, et al. Dosimetric characterization of medical linear accelerator Photon and Electron beams for the treatment accuracy of cancer patients. World Journal of Advanced Engineering Technology and Sciences. 2021;3(1):041–059.

[8] Varatharaj C, Shwetha B, Reddy RB, et al. Physical characteristics of photon and electron beams from a radiotherapy accelerator. International Journal of Medical Research and Review. 2016;4(7).

[9] Roy S K, Das P K, Khatun R, Md. et al. Dosimetric Characteristics of 6 MV Medical Linac at BAEC. International Journal of Medical Physics, Clinical Engineering and Radiation Oncology. 2021;10:38– 46.

[10] Chowdhury R I, Rabby F, Ahmed R, et al. Beam profile characteristics of a Varian linear accelerator across different photon energy levels. International Journal of Science and Research Archive, 2024, 12(02), 1072–1082. Article DOI: https://doi.org/10.30574/ijsra.2024.12.2.1316

[11] Chowdhury R I, Rabby F, Ahmed R, et al. A comparative study of photon beam percentage depth dose of a recently installed varian vitalbeam linear accelerator at TMSS cancer center, Bangladesh. Int J Radiol Radiat Ther. 2024;11(4):100–104. DOI: 10.15406/ijrrt.2024.11.00394